Longitudinal and Lateral Dynamics Control: PI and MPC Implementation for Vehicle Modelling and Control

Smart Transportation (WEUMST0)

18th December 2024

Iñaki Román

Nomenclature

$\dot{\psi}$ Yaw rate of the vehicle (rad/s)

λ Slip ratio, representing wheel-ground dynamics

μ_1, μ_2, μ_3 Friction coefficients for different terrains

ω Angular speed of the wheel (rad/s)

θ Road slope angle (rad)

$C_{\alpha_f}, C_{\alpha_r}$ Lateral stiffness coefficients for front and rear tires (N/rad)

C_λ Longitudinal stiffness of the tire (N)

F_d Drag force acting against vehicle motion (N)

F_r Rolling resistance force (N)

F_x Longitudinal force acting on the vehicle (N)

$F_{\max}$ Maximum force limited by friction (N)

g Gravitational acceleration ($9.81\,\mathrm{m/s^2}$)

m Mass of the vehicle (kg)

R Radius of the wheel (m)

T Torque applied to the wheels (Nm)

v_x Longitudinal velocity of the vehicle (m/s)

y Lateral position of the vehicle (m)

Contents

1 Abstract

This laboratory explores the principal control systems that are applied in automotive dynamics, focusing on the design and implementation of a longitudinal and lateral controllers for the dynamics of the Renault Megane vehicle, this laboratory emphasizes the difference between a nonlinear and linearized models for the control design. Furthermore, the longitudinal control is implemented using a PI controller with anti-Windu mechanism and feedforward control. For the lateral dynamics of the car, a Model Predictive Control (MPC) is designed to the nonlinear simulation environment, giving a reference trajectory based on the Montmelo racetrack path. This lab englobes a comprehensive understanding of automotive control systems by combining the theory with simulation in MATLAB/Simulink and testing under diverse scenarios, including road friction and slope variations.

2 Introduction

This laboratory focuses on the modelling, simulation and control architecture of the vehicle dynamics that will emphasize on longitudinal and lateral forces. The primary objectives are to design controllers for speed regulation and yaw rate tracking while taking into account the non-linear dynamics inherent in real-world automotive systems. For this laboratory, we will use the properties of the Renault Mégane that will provide a realistic framework for simulation and testing.

For the longitudinal dynamics, a Proportional-Integral (PI) controller is implemented in order to regulate the vehicle's linear speed. The key steps include:

- Derive the non-linear model for the longitudinal force model of the vehicle from the vehicle properties and equations of movement.
- Incorporate the non-linear effects that affect the vehicle, such as drag force F_d, road slope θ, terrain friction coefficients (μ_1, μ_2, μ_3), and the wheel angular speed ω, using the Buck-Hardt model for the slip ratio λ.
- Evaluate the controller performance using saturation limits $F_{\max}$ and anti-windup mechanisms.

For the lateral dynamics of the vehicle, a Model Predictive Control (MPC) controller is designed to track the yaw rate ($\dot{\psi}_{\text{ref}}$) while the controller can minimize addressing steering. The MPC framework works accordingly to dynamically to longitudinal speed changes, ensuring the stability of the vehicle across different conditions and manoeuvres.

The final part involves combining the longitudinal PI and the lateral MPC controllers into one system, tested on a simulation of the Montmelo racetrack. We will add variations in road conditions (dry, wet, cobblestone or ice surfaces) and different speed references are given to the controller to test its robustness.

This lab provides hands-on experience with advanced control techniques and a deeper understanding of the vehicle dynamics, highlighting the relationship between the linearized models of control design and the nonlinear models for simulation and how different controllers act upon real world applications.

3 Objectives

The primary objectives of the lab session are:

1. Derivation of the longitudinal non-linear force model based on vehicle dynamics.
2. Incorporation of non-linear effects, including drag force, road slope, terrain friction coefficients, and wheel angular speed.
3. Implementation of a longitudinal control system using a PI controller.
4. Evaluation of the controller performance with saturation limits and anti-windup mechanisms.
5. Design and implementation of a lateral control system for yaw rate tracking using Model Predictive Control (MPC).
6. Integration of longitudinal and lateral controllers in a unified vehicle control framework.
7. Simulation of vehicle dynamics under varying scenarios on the Montmelo racetrack.
8. Analysis of controller robustness under diverse terrain conditions and speed profiles.

4 Methodology

4.1 Vehicle Dynamics Modelling

4.1.1 Bicycle model

For this laboratory is used the bicycle model [1] as a simplified representation of a four-wheel vehicle that is used to analyse the longitudinal and lateral behaviour. This model has a reduced complexity of the system by approximating the front and back wheel properties while preserving the essential dynamics used for control architecture and simulation.

The key assumptions of the bicycle model is that it assumes small steering angles and flat road surfaces furthermore, the lateral motion of the vehicle is perpendicular to the heading direction and the yaw motion is around its vertical axis. The bicycle model is better to define with the following figure 1:

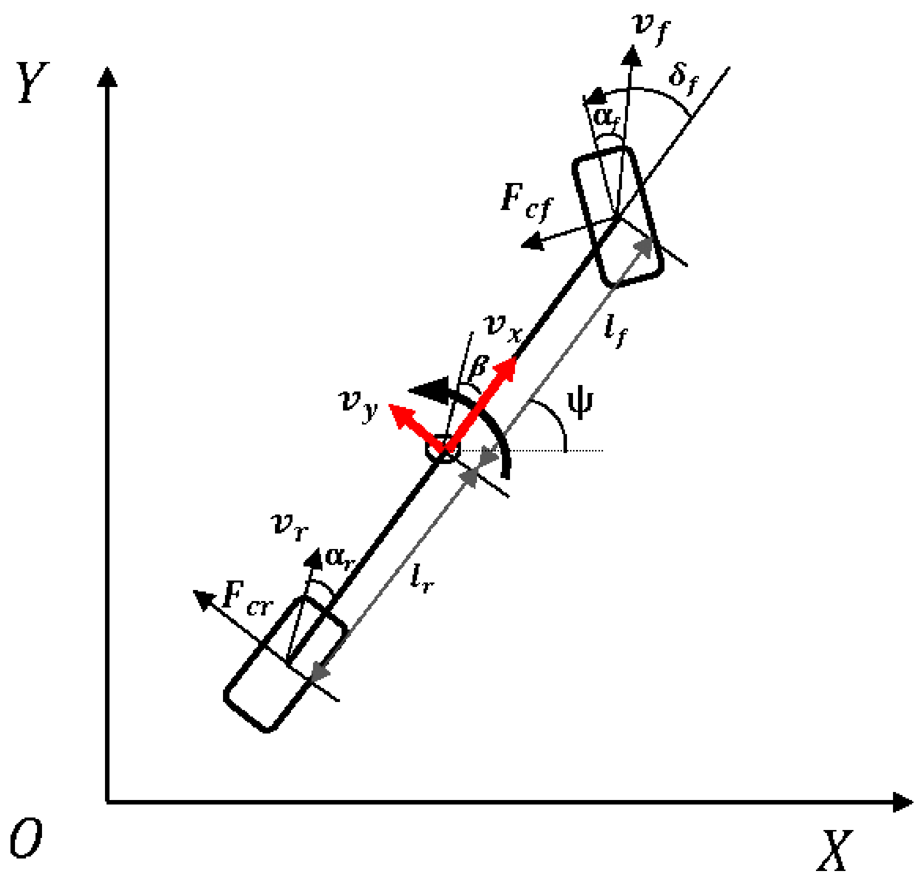

Figure 1: Dynamic bicycle model.

This model captures the forces acting on the vehicle, ground interaction and the non-linear effects that act on the car's motion. The following equations are given to develop and implement in simulation and later test with the controllers:

4.2 Linear longitudinal Vehicle Dynamics Modelling

4.2.1 Linear Longitudinal Force Model

The longitudinal lineal force F_x comes from the vehicle's properties and equations of motion, it signifies total energy generated in the longitudinal axis of the vehicle and is influenced by several factors like Vehicle mass (m), Aerodynamic Drag (F_d), rolling resistance (F_{rr}), Friction Force (F_{fric}), road slope (θ) and many more, nonetheless for the first iteration of the longitudinal model the equation is used a simplified linear model given by 1:

$$F_x = C_\lambda \cdot \lambda \tag{1}$$

Where C_λ is the Longitudinal stiffness of the tire and λ is the slip ratio that represents the difference between the actual tire speed and the ground speed of the vehicle on the longitudinal axis. The equation 1 describe the longitudinal force F_x as a linear relationship, note that this representation is only valid for small slip conditions of (λ), in the next section it would be discussed a non-linear model "Pacejka" for vehicle dynamics that capture's more complex behaviour of the vehicle.

4.2.2 Slip Ratio

The slip ratio λ is the motion between the wheel and the ground, is an important parameter in the analysis of the tire-road interaction. The equation 2 reflects the difference between the wheel's rotational speed and the longitudinal velocity of the vehicle, it is important to note that a zero slip ratio denotes that the tire is not rolling but slipping.

For this laboratory, the slip ratio is calculated using the Buck-Hardt model, which defines λ different depending on if the vehicle is accelerating or braking:

$$\lambda = \begin{cases} \frac{R\omega - v_x}{v_x} & \text{for braking,} \\ \frac{R\omega - v_x}{R\omega} & \text{for acceleration.} \end{cases} \tag{2}$$

Where R is the Effective tire radius, ω the angular velocity of the wheel and v_x the longitudinal velocity of the vehicle.

4.2.3 Drag Force

The drag force F_d represents the total resistance acting on the vehicle as it moves through air and interacts with the road. it is an important component of the longitudinal dynamics of the vehicle, and it is composed of the aerodynamic drag and rolling resistance. The overall drag force is given by equation 3:

$$F_d = \frac{1}{2}\rho C_d A_f v_x^2 + C_r m g \cos\theta \tag{3}$$

- ρ: Air density (kg/m^3).
- C_d: Drag coefficient, determined by the vehicle's aerodynamic design.
- A_f: Frontal area of the vehicle (m^2).
- v_x: Longitudinal velocity of the vehicle (m/s).
- C_r: Rolling resistance coefficient.
- m: Vehicle mass (kg).
- g: Gravity (9.81 m/s^2).
- θ: Road slope angle (radians).

As observed, the drag force equation has two terms. The Aerodynamic Drag, ($\frac{1}{2}\rho C_d A_f v_x^2$) which is the proportional to the square of the vehicle's speed v_x, making it more apparent in high speeds. And the rolling resistance ($C_r m g \cos\theta$) that is influenced by the vehicle's weight and road surface conditions.

4.2.4 Simulation of the longitudinal linear system

To analyse the behaviour of the longitudinal linear system, a Simulink model was modelled to simulate the vehicle's dynamics. This model incorporates the equations governing the longitudinal, slip angle and drag force models, focusing on the relationship of velocity, acceleration and external forces like the drag force.

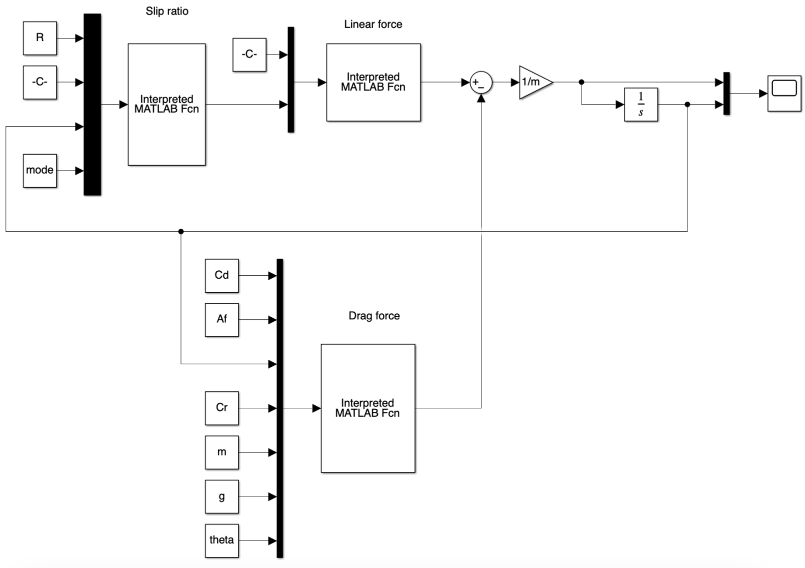

Figure 2: Schematic of the linear model in Simulink.

The simulation results are presented in the form of a graph that displays the acceleration and the velocity of the vehicle over time. These elements help to evaluate the system's response under the simple linear model.

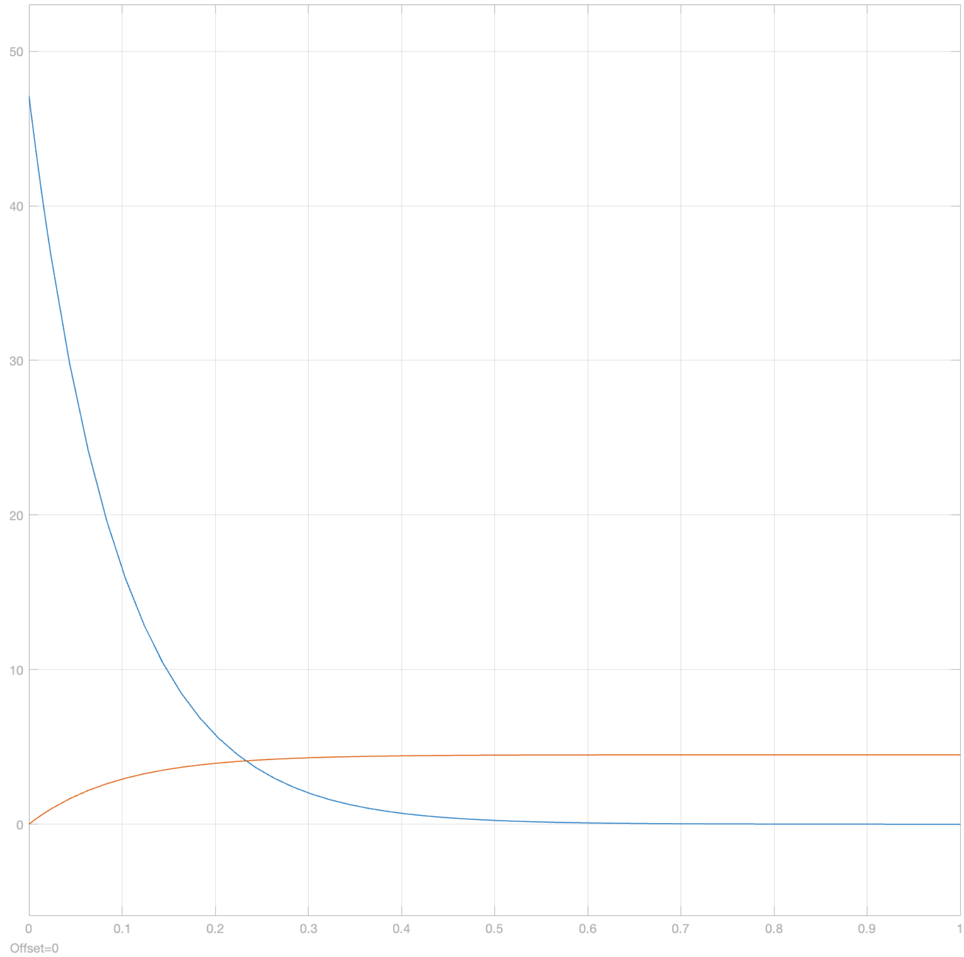

Figure 3: Simulation of the linear model in Simulink.

The Simulink structure is shown in Figure 2, and the corresponding graph of acceleration and velocity is presented in Figure 3. From the simulation, it can be observed that the vehicle's acceleration, represented in yellow, starts at a high value and decreases rapidly, stabilizing at 0 m/s. Meanwhile, the vehicle's velocity, represented in blue, begins at 0 m/s and rises to 5 m/s . The velocity increases rapidly at first, but then levels off due to the drag force, which grows with the velocity. At 5 m/s , the forces acting on the system reach equilibrium, resulting in no further acceleration.

4.3 Non-Linear Longitudinal Force Model

The longitudinal force F_x comes from the vehicle's model and equations of motion, while the linear model $F_x = C_\lambda \cdot \lambda$ provide a simpler model it can be only used for small slip ratios and low velocities. For a more realistic representation is used a non-linear model where is influenced by more factors such as aerodynamic drag (F_d) and more realistic friction coefficient μ_λ, the non-linear longitudinal model is defined by the product of the normal force acting on the tire (F_n) and μ_λ as shown in the equations 4 and 5:

$$\mu_\lambda = \text{sign}(\lambda) \cdot \left(\mu_1 \cdot \left(1 - e^{-|\lambda| \cdot \mu_2}\right) - |\lambda| \cdot \mu_3\right), \tag{4}$$

$$F_x = \mu_\lambda \cdot F_n \tag{5}$$

- μ_1: Peak friction coefficient.
- μ_2: Exponential decay rate.
- μ_3: Linear decay term.
- λ: Slip ratio.

4.3.1 Simulation of the longitudinal non-linear system

In order to analyse the behaviour of the longitudinal non-linear model, a Simulink simulation was created to analyse the vehicle dynamics. This formulation includes Pacejka's Equation, slip ratio and the drag force. The formulation of the system is modelled in 4

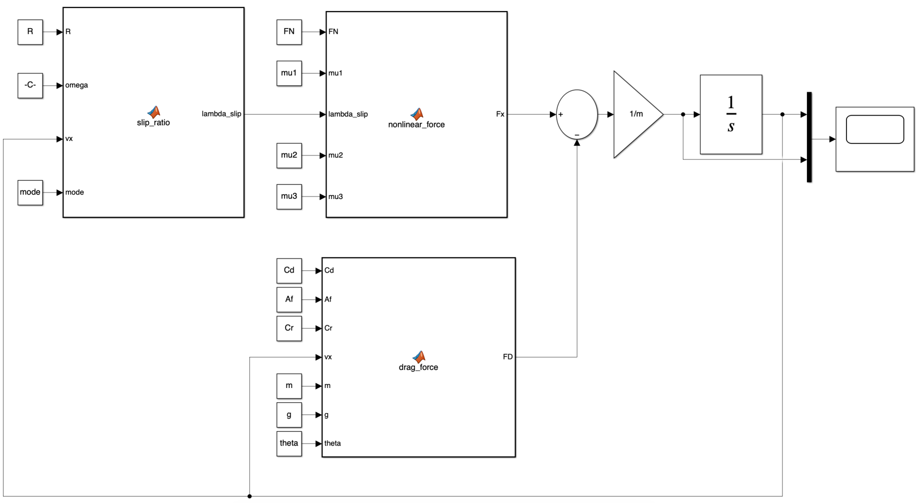

Figure 4: Schematic of the non-linear model in Simulink.

The simulations results are presented on fig 5 that displays the acceleration and velocity of the vehicle over time. It can be observed that a different pattern on the acceleration of the vehicle with the non-linear model, this is because the equation is a better approximation to the real vehicle.

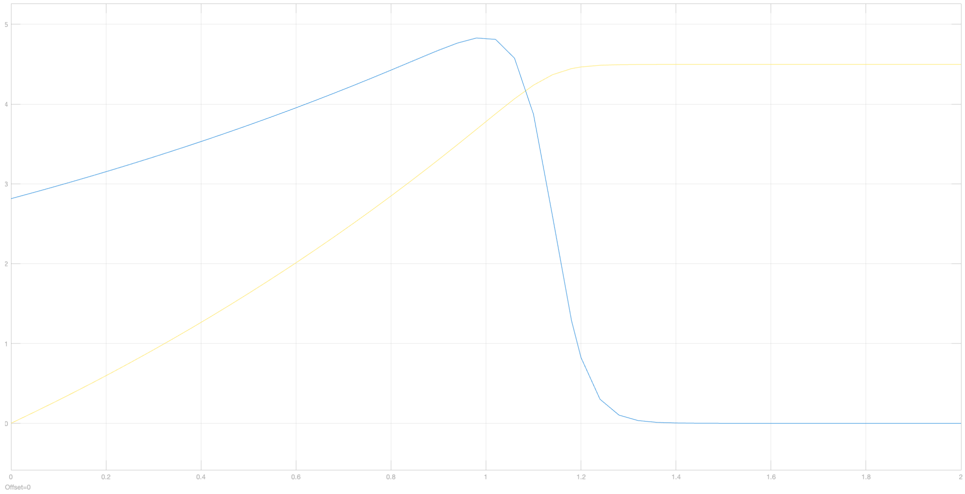

Figure 5: Simulation of the non-linear model in Simulink.

4.3.2 Maximum Force Saturation

A saturation limit $F_{\max}$ is defined based on the terrain's friction coefficients:

$$F_{\max} = \mu \cdot F_N,$$

where $F_N = mg\cos\theta$ is the normal force.

4.3.3 Wheel Speed Conversion

The overall speed of the vehicle V_x is a longitudinal motion, and it is linked to the angular speed of the wheel ω and the slip ratio λ using the equations below:

$$\omega = \begin{cases} \frac{v_x(1+\lambda)}{R} & \text{for braking,} \\ \frac{v_x(1-\lambda)}{R} & \text{for acceleration.} \end{cases}$$

4.4 Control System for Longitudinal Dynamics

To regulate the vehicle's longitudinal velocity v_x, a Proportional-Integral (PI) controller was designed. The control law is given by:

$$T(s) = K_p + \frac{K_i}{s},$$

where K_p is the proportional gain and K_i is the integral gain. Anti-windup mechanisms and saturation limits were implemented to handle integrator wind-up and ensure stability.

$$C(s) = 3371.8 + \frac{1668.70}{s} \tag{6}$$

The Longitudinal model with the integration of a PI controller can be developed in Simulink using the PID controller block as seen in 6:

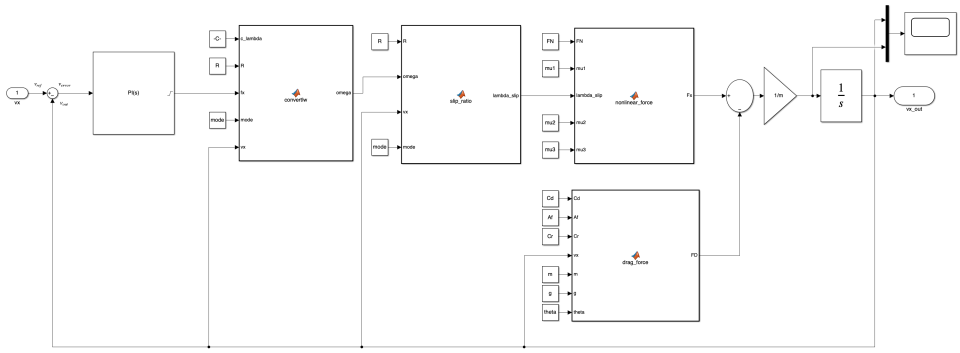

Figure 6: Simulink diagram of the longitudinal model including the PI controller.

The simulation of the controller are presented in 7 that display reference velocity of $10 m/s$. It can be observed that the controller is working correctly and with the implementation of the saturation it doesn't have big output references and no overshoot.

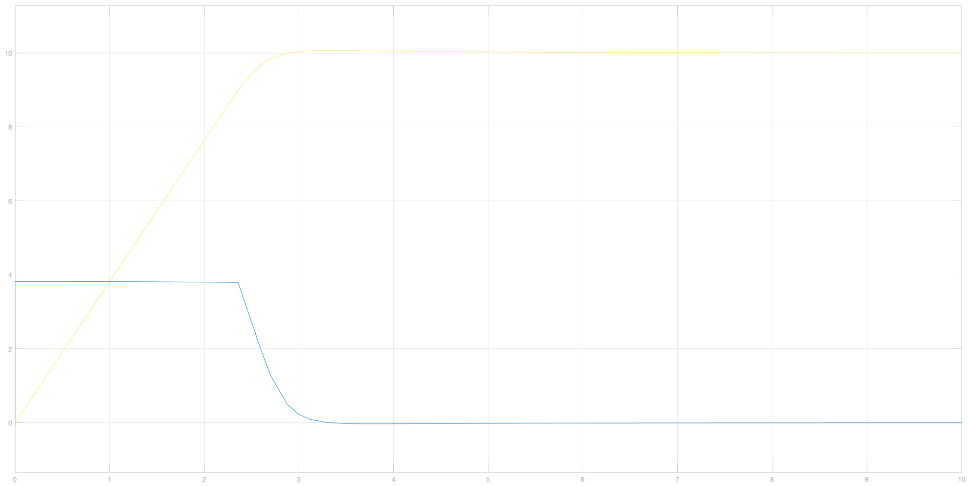

Figure 7: Simulation of the PI controller in the longitudinal system.

4.5 Lateral Vehicle dynamics

The lateral dynamics of the vehicle is an important part for determining the stability and manoeuvrability. This section analyses and synthesis the behaviour of the system when is subject to lateral forces, focusing on the main parameters influencing the response, including the vehicle heading angle, tyres angle and steering angle.

4.5.1 Lateral force dynamics

The lateral dynamics are given by the simplified bicycle model given before. The key equations on the lateral model are based on the relationship between the yaw rate ($\dot{\psi}$), tyre side-slip angle (β), lateral velocity (v_y) and the steering angle (δ). These dynamics are also influenced by the physical parameters of the vehicle, such as tire cornering stiffness, vehicle mass and velocity. Given that the vehicle can only turn with the front wheels, the force interacting will be different, the calculation of the forces are given by the Pacejka's Equation: 7, 8, 9 and 10:

$$\alpha_f = \delta - \arctan\left(\frac{v_x \cdot \beta + l_f \cdot \dot{\psi}}{v_x + \epsilon}\right) \tag{7}$$

$$\alpha_r = -\arctan\left(\frac{v_x \cdot \beta - l_r \cdot \dot{\psi}}{v_x + \epsilon}\right) \tag{8}$$

$$F_{yf} = D_y \cdot \sin\left(C_y \cdot (B_y \cdot (1 - E_y) \cdot \alpha_f + E_y \cdot \arctan(B_y \cdot \alpha_f))\right) \cdot \exp\left(-6 \cdot |\lambda|^5\right) \tag{9}$$

$$F_{yr} = D_y \cdot \sin\left(C_y \cdot (B_y \cdot (1 - E_y) \cdot \alpha_r + E_y \cdot \arctan(B_y \cdot \alpha_r))\right) \cdot \exp\left(-6 \cdot |\lambda|^5\right) \tag{10}$$

With:

$$B_y = 2(2 - \mu)8.3278 \tag{11}$$

$$C_y = (5/4 - \mu/4)1.1009 \tag{12}$$

$$D_y = \mu 2268 \tag{13}$$

$$E_y = -1.1661 \tag{14}$$

4.5.2 Yaw equation

The dynamic equation that represents the heading angle of the vehicle is given by equation 15, which describes how the change of force in the tyres affects the rate of turn of the vehicle that also depends on the distance of the tires to the centre of the vehicle.

$$\dot{\psi} = \frac{F_{yf} \cdot l_f - F_{yr} \cdot l_r}{I_z} \tag{15}$$

4.5.3 Side-slip angle equation

The dynamic equation that represents the difference of the rate of change of the tire's direction given the change of the direction of the vehicle is given by the side-slip angle equation 16.

$$\dot{\beta} = \frac{F_{yf} + F_{yr}}{m \cdot v_x} - \dot{\psi} \tag{16}$$

4.5.4 Simulation of the Lateral Dynamics

The simulation of the lateral model was done in Simulink/MATLAB, giving as an input a steering angle of 0.3 radians or 17°. Also, a function is developed to calculate the vehicle position given the linear longitudinal velocity, the yaw and side-slip angle using the kinematic model.

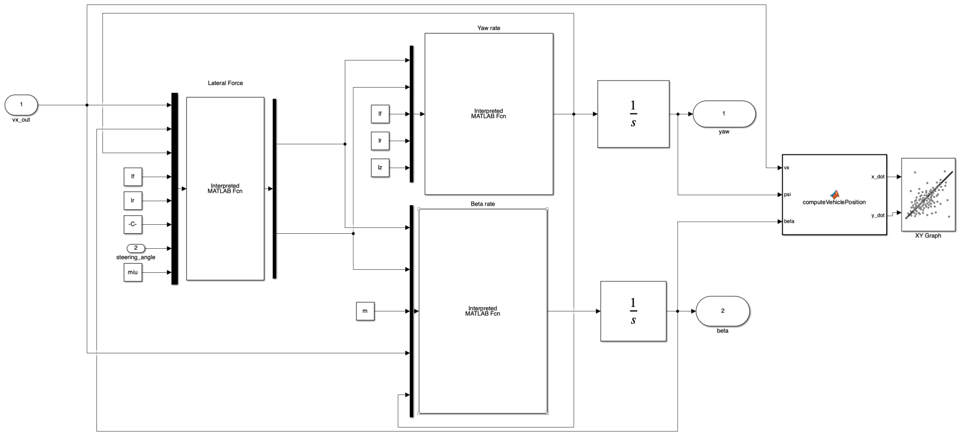

Figure 8: Lateral model of the vehicle in Simulink.

The results of the simulation are given by fig 9 where it can be observed that the simulated vehicle is turning more and more as the simulation time increases, this is because the constant steering input doesn't change, thus the vehicle keeps turning at the same rate.

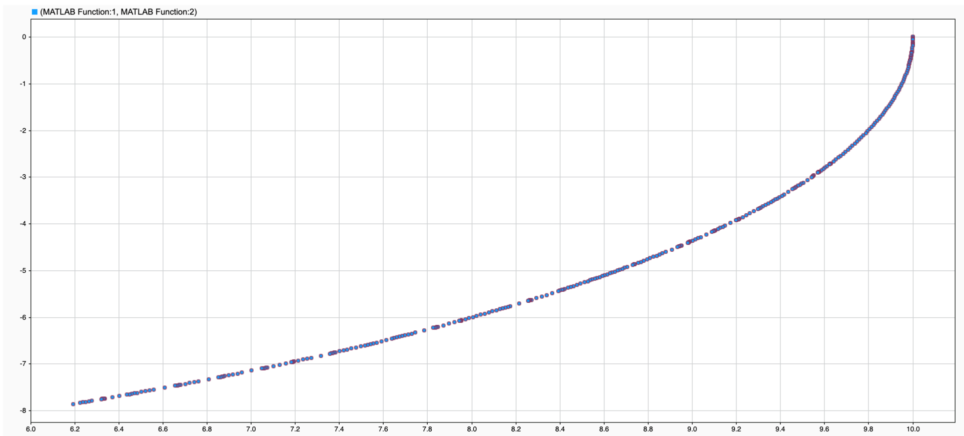

Figure 9: Simulation of the lateral model of the vehicle in Simulink.

4.6 Model Predictive Control for the Lateral Dynamics

The previously presented simulation represents an open-loop system without a controller to provide the necessary reference for accurately steering the vehicle. For this, a Model Predictive Controller (MPC) [3] is designed using MATLAB's Model Predictive control Toolbox and state space representation of the lateral motion is given by equation 17, where the input for the system is given by the steering angle (δ), the state of the system ($v_y, \dot{\psi}$) and the outputs ($\dot{v_y}, \ddot{\psi}$) [2]. Note that for the dynamics of the system is considered v_x and can be changed over time, for simplicity when linearizing the model and simulation $v_x = 10 m/s$.

$$\begin{bmatrix} \dot{v_y} \\ \ddot{\psi} \end{bmatrix} = \begin{bmatrix} \frac{-C_f + C_r}{mV_x} & -V_x + \frac{C_r L_r - C_f L_f}{mV_x} \\ \frac{-L_f C_f + L_r C_r}{I_z V_x} & \frac{-L_f^2 C_f + L_r^2 C_r}{I_z V_x} \end{bmatrix} \begin{bmatrix} v_y \\ \dot{\psi} \end{bmatrix} + \begin{bmatrix} \frac{C_f}{m} \\ \frac{L_f C_f}{I_z} \end{bmatrix} \delta \tag{17}$$

The implementation of the MPC is given by the figure 10:

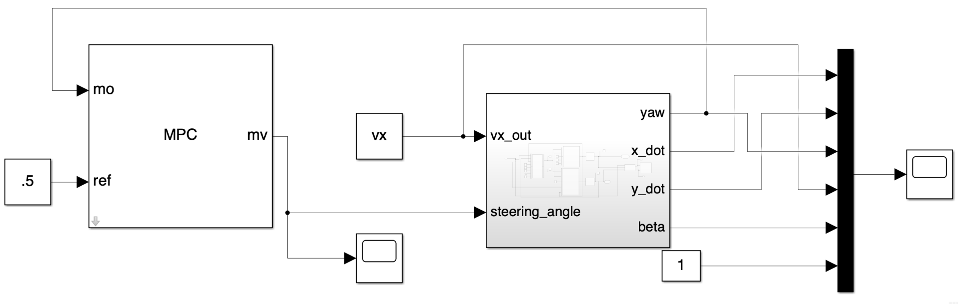

Figure 10: Implementation of MPC controller in Simulink.

And the performance of the MPC controller in figure 11, where it can be observed that the controller follows the reference of 0.5 radians.

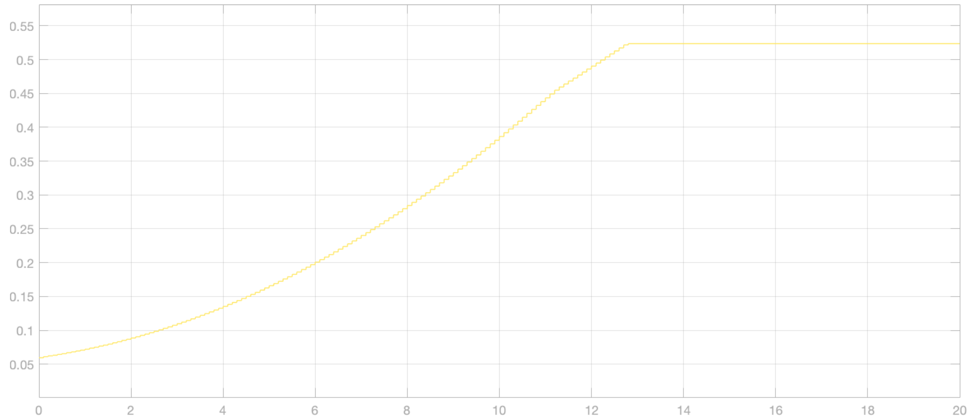

Figure 11: Simulation of MPC controller in Simulink.

5 Simulation on the Montmelo racetrack

The longitudinal and lateral models, along with their respective controllers, were integrated, with the lateral model relying on the linear velocity (v_x) provided by the longitudinal model. Additionally, the pure pursuit algorithm [4] was implemented to supply the system with the necessary input variables for defining the track trajectory and tracking error. The Simulink implementation of this complete system is shown in Figure 12.

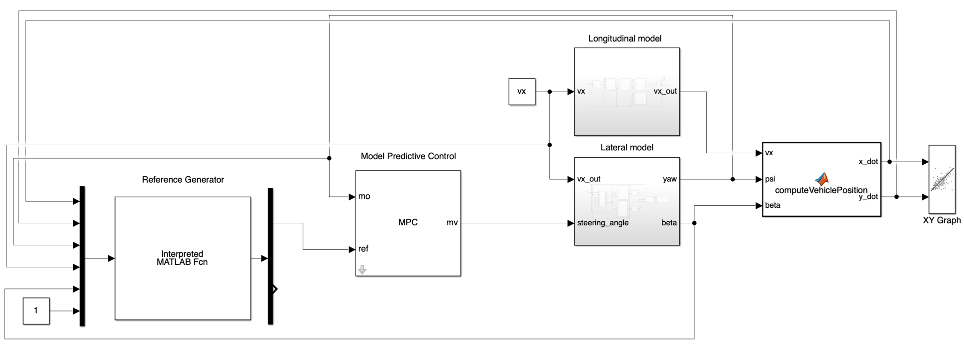

Figure 12: Complete simulation of the vehicle and control.

The Montmelo racetrack is given by figure 13:

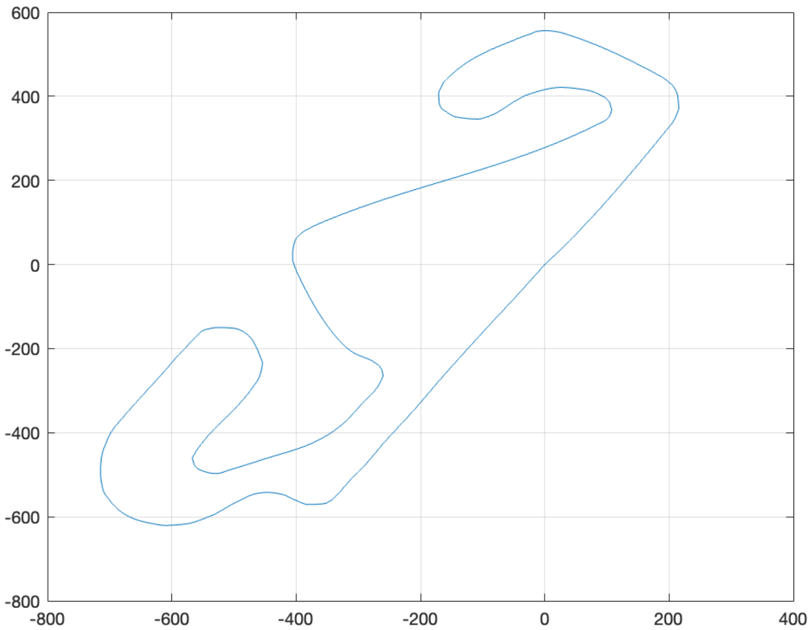

Figure 13: Montmelo race track.

Due to challenges in the final integration of the vehicle dynamics with the pure pursuit algorithm, the controllers could not be tested on the Montmelo racetrack. Additionally, issues with algebraic loops in the feedback of the longitudinal and lateral dynamics complicated the overall system simulation. Nonetheless, the complete model was tested with a fixed yaw rate reference for the MPC controller and a fixed linear velocity for the PI controller. The results of the simulation for the entire vehicle dynamics are presented in Figure 14:

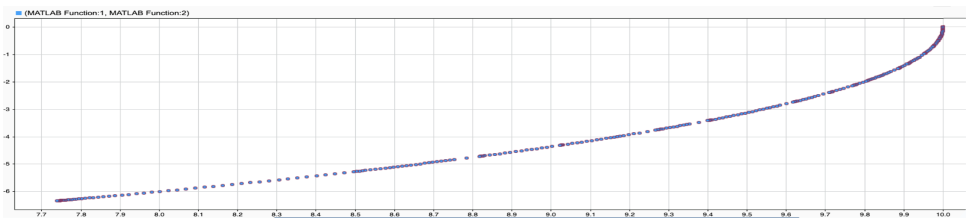

Figure 14: Simulation of the complete system.

6 Conclusions

This laboratory provides a comprehensive study of longitudinal, lateral dynamics and control, focusing on the design, simulation and implementation of control systems for a realistic vehicle model. Through the application of a Proportional-Integral (PI) and Model Predictive Control (MPC) methods, the system demonstrated significant potential for regulating longitudinal velocity and tracking the yaw rate, respectively.

The linear and nonlinear models were developed for longitudinal dynamics highlighted the critical physical phenomenons like tire-road interaction, drag forces, and slip ratios. The PI controller, enhanced with an anti-windup mechanisms, effectively managed the vehicle's acceleration and velocity, even varying the terrain and slope conditions.

For the lateral dynamics, the bicycle model served as a simplified model for the vehicle and analyse the yaw rate and steering behaviour. The MPC controller proved of maintaining stability and tracking to the desired reference. Despite challenges in integrating the pure pursuit algorithm with the vehicle dynamics model, a fixed yaw rate reference allowed the complete system to be tested successfully.

The simulation on the Montmelo racetrack, while not successful due to algebraic loop issues, provided a valuable insights into the system's behaviour under realistic conditions. The results emphasized the importance of a robust integration framework for longitudinal and lateral controllers, as well as the need for advanced tuning to address the nonlinearities and high-speed change in dynamics.

Overall, this laboratory joined the theoretical concepts with practical implementation, offering a deeper understanding of automotive control systems. Future work could focus on resolving the integration challenges, extending the pure pursuit algorithm for dynamical trajectory tracking, and testing the system under more realistic conditions to validate its performance further.

References

[1] Game-based lateral and longitudinal coupling control for autonomous vehicle trajectory tracking, 2024. Scientific Figure on ResearchGate. Available from: `https://www.researchgate.net/figure/Dynamic-bicycle-model_fig1_357040239` [accessed 9 Dec 2024].

[2] BE Mechatronic Systems Control. Vehicle lateral dynamics control: Trajectory tracking problem, 2024. Path planning and lateral force analysis exercises.

[3] J. Löfberg. Yalmip: A toolbox for modeling and optimization in matlab. *YALMIP Documentation*, 2004. Accessed 2024.

[4] Olivier Sename and Anis Koliai. Pure pursuit generator. `https://chamilo.grenoble-inp.fr/main/document/document.php?cidReq=ENSE3WEUMST0&id_session=0&gidReq=0&gradebook=0&origin=`, Dec 2024. Provided in class through the classroom website.

A Vehicle Parameters

Table 1: Renault Megane Parameters Used in the Simulation

Parameter	**Value (S.I.)**
Mass (m)	1400 kg
Moment of inertia (I_z)	1960 kg·m^2
Distance to front axle (l_f)	1.177 m
Distance to rear axle (l_r)	1.358 m
Drag coefficient (C_d)	0.35
Frontal area (A_f)	2.14 m^2
Rolling resistance coefficient (C_r)	0.015
Wheel radius (R)	0.3 m
Longitudinal stiffness (C_λ)	66100 N/rad
Front lateral stiffness ($C_{\alpha f}$)	84085 N/rad
Rear lateral stiffness ($C_{\alpha r}$)	87342 N/rad

B Road Conditions

Table 2: Road Surface Friction Coefficients (μ)

Surface Type	μ_1	μ_2	μ_3
Dry (Asphalt)	1.11	23.99	0.52
Wet (Asphalt)	0.687	33.822	0.347
Cobblestone	1.37	6.46	0.67
Ice	0.19	94.13	0.06